BIOLOGY OF REPRODUCTION (2014) **90**(1):16, 1–13
Published online before print 4 December 2013.
DOI 10.1095/biolreprod.113.111831

SPACA7 Is a Novel Male Germ Cell-Specific Protein Localized to the Sperm Acrosome That Is Involved in Fertilization in Mice[1]

Edward B. Nguyen,[3] Andrew D. Westmuckett,[4] and Kevin L. Moore[2,3,4,5,6]

[3]*Department of Cell Biology, University of Oklahoma Health Sciences Center, Oklahoma City, Oklahoma*
[4]*Cardiovascular Biology Research Program, Oklahoma Medical Research Foundation, Oklahoma City, Oklahoma*
[5]*Department of Medicine, University of Oklahoma Health Sciences Center, Oklahoma City, Oklahoma*
[6]*Oklahoma Center of Medical Glycobiology, University of Oklahoma Health Sciences Center, Oklahoma City, Oklahoma*

ABSTRACT

Sperm acrosome associated 7 (SPACA7) is a novel protein of unknown function with no homology to any known protein. *Spaca7* transcripts are detected only in testis and predict a 158-residue mature polypeptide with one potential N-glycosylation site and no cysteines. Orthologs are present in various species, including mice and humans. We developed a polyclonal antibody to mouse SPACA7 to study its expression and function. Western blotting and immunofluorescence microscopy detected SPACA7 only in testis, and it was detected in testis starting at Postnatal Day 21 and into adulthood. Immunofluorescence staining of testicular germ cells detected weak SPACA7 expression as early as zygotene spermatocytes. Higher expression was observed in round spermatids, where SPACA7 was localized to a perinuclear spot adjacent to the Golgi and to the acrosome of elongating spermatids and spermatozoa. Immunogold electron microscopy demonstrated that SPACA7 is localized within the proacrosomal granule of round spermatids and the acrosome of spermatozoa. Finally, we showed that SPACA7 was retained within the acrosome of epididymal sperm and was released upon the acrosome reaction. To assess if SPACA7 was involved in fertilization, in vitro fertilization assays in the presence of anti-SPACA7 IgG were performed. Anti-SPACA7 inhibited fertilization of cumulus-intact eggs and prominently delayed cumulus dispersal. However, anti-SPACA7 did not inhibit fertilization of cumulus-free eggs. Our findings indicate that release of SPACA7 from the acrosome accelerates cumulus dispersal and facilitates fertilization via unknown mechanisms. This study is the first to document the expression of endogenous SPACA7 and a function for this novel acrosomal protein.

acrosome, cumulus cells, fertilization, sperm, testis

INTRODUCTION

The events that are required to generate sperm capable of fertilizing an egg are extraordinarily complex [1]. In mammals, these include events in the hypothalamus, pituitary, testis, epididymis, and in the female genital tract and involve a myriad of proteins, signaling pathways, cell-cell interactions, and cellular components. After germ cells progress through the successive stages of meiosis and spermiogenesis in the testis, they enter the epididymis as immotile cells that are incapable of fertilization. In the epididymis they become motile and fertilization competent cells in a complex process called maturation. The latter process is triggered and influenced by the complex and changing lumenal microenvironment to which sperm are exposed during epididymal transit. After mating and ejaculation, sperm must then undergo capacitation, migrate to the site of fertilization, and then penetrate the cumulus oophorus and zona pellucida in order to successfully fuse with the oolemma.

Our understanding of spermatogenesis, the processes in the epididymis and female reproductive tract that prepare sperm for fertilization, and the events surrounding fertilization per se has grown steadily in recent years. However, these processes are extremely complicated, and many details remain poorly understood. For example, transcript profiling of male germ cells from mice reported by Schultz et al. [2] identified 1652 genes whose expression increased markedly at the onset of meiosis, and ≈20% of these genes are expressed only in the male germ line. These authors went on to estimate that ≈4% of the mouse genome (>2300 genes) is expressed in postmeiotic male germ cells. However, many of these genes remain unannotated.

In previous unpublished work, we identified a novel protein called hypothetical protein LOC78634 in mouse epididymis that attracted our interest and prompted the current study of its expression and potential function(s). First, high-throughput gene expression profiling of a diverse array of normal mouse tissues, organs, and cell lines reported at BioGPS.org [3] showed that transcripts were detected only in testis [4]. This is consistent with the EST profile in Unigene (Mm.116871). Notably, this gene was not identified in the study by Schultz et al. [2] because it was not represented on the Affymetrix array set used. Second, it had no homology to known proteins, and its function(s) was unknown. Third, at the time we initiated this study, *1700094C09Rik*, the gene encoding hypothetical protein LOC78634, was not annotated, and there were no published data about this protein.

During the course of this work, *1700094C09Rik* was assigned the gene name *Spaca7* based on a paper by Korfanty et al. [5], who reported that SPACA7 was an acrosomal protein. However, this study has several significant shortcomings. Most importantly, no data were presented on expression and localization of the endogenous mouse SPACA7 protein. Although immunocytochemical data suggesting that acrosomal localization in human sperm was provided, an uncharacterized

[1]Supported in part by National Institute of Health Grant HD056022 (to K.L.M.) and institutional funds from the Oklahoma Medical Research Foundation. Presented in part at the 38th Annual Meeting of the American Society of Andrology, 13–16 April 2013, San Antonio, Texas.
[2]Correspondence: Kevin L. Moore, Oklahoma Medical Research Foundation, 825 Northeast 13th St., Oklahoma City, OK 73104.
E-mail: kevin-moore@omrf.org

Received: 28 June 2013.
First decision: 29 July 2013.
Accepted: 27 November 2013.

eISSN: 1529-7268 http://www.biolreprod.org
ISSN: 0006-3363

polyclonal antibody of unproven specificity was used, and the images provided were not convincing. Furthermore, their conclusion that mouse SPACA7 was localized to the acrosome was based solely on the localization of EGFP fluorescence in transgenic mice overexpressing a SPACA7-EGFP fusion protein. The promoter element used was a nonnative promoter from the rat *Hspa2* gene that drives expression not only in male germ cells but also in a variety of extratesticular tissues [6]. In addition, the authors showed that the transgene was expressed as early as Postnatal Day 15 (P15), while endogenous *Spaca7* transcripts do not appear until P21.

In this study, we performed a detailed analysis of the expression of endogenous SPACA7 in the mouse using a well-characterized polyclonal antibody. We report on the developmental onset expression of SPACA7, as well as its tissue, cellular, and subcellular localization, using a combination of subcellular fractionation, Western blotting, immunofluorescence microscopy, and immunogold electron microscopy. Most importantly, we provide the first evidence documenting a role for SPACA7 in fertilization.

MATERIALS AND METHODS

Ethics Statement

All procedures involving vertebrate animals were reviewed by the Institutional Animal Care and Use Committee at the Oklahoma Medical Research Foundation (protocol no. 10–19) and were performed in accordance with the eighth edition of the *Guide for the Care and Use of Laboratory Animals* (NRC 2011).

Animals

All experiments except the in vitro fertilization studies were performed using 129S6/SvEvTac mice (Taconic Farms). For in vitro fertilization studies, 6- to 8-wk-old NSA (CF-1) female egg donors and ICR (CD-1) male retired breeder sperm donors were purchased from Harlan Laboratories. Animals were housed and fed as previously described [7].

Materials

FITC-conjugated goat anti-rabbit IgG (#F0382), human chorionic gonadotropin (hCG; #C0163), and Type I-S bovine testes hyaluronidase (545 units/mg; #H3506) were purchased from Sigma-Aldrich. Anti-Syntaxin 6 (SYN6) mAb 3D10 (mouse IgG_1; #ab12370), anti-synaptonemal complex protein 3 (SYCP3) mAb Cor 10G11/7 (mouse IgG_1; #ab97672), and DyLight 594-conjugated goat anti-mouse IgG (#ab96881) were purchased from Abcam. Rhodamine-conjugated *Arachis hypogaea* lectin (peanut agglutinin [PNA]; #RL-1072), HRP-conjugated goat anti-rabbit IgG (#PI-1000), and Vectashield hard set mounting medium with DAPI were from Vector Laboratories. Equine chorionic gonadotropin (eCG; #367222) and EmbryoMax human tubal fluid (HTF; #MR-070-D) was purchased from EMD Millipore.

Methods

Production of Antiserum to SPACA7. The coding sequence for the putative mature polypeptide for mouse SPACA7 (Gln^{25}-Phe^{182}) was amplified by PCR from a full-length SPACA7 cDNA (accession no. CA465939, clone ID 6774242) purchased from Open Biosystems using *Taq* polymerase (Qiagen). The forward primer 5′-AGA TAT ACC ATG GGC CAG CCG ATC AAG ACA ACT TCA-3′ added an *NcoI* site (underlined), and the reverse primer 5′-GTG GTG GTG CTC GAG AAA GAT GCT TTC TGT TAG CTC-3′ added an *XhoI* site (underlined) to the amplicon. The amplified fragment was directionally cloned into the pET28a vector (Novagen) that added a His_6-tag to the C terminus, and the vector sequence was confirmed. The purified vector was used to transform BL21 (DE3) *E. coli* (Novagen). Production of the recombinant protein was induced by 1 mM isopropyl β-D-thio-galactopyranoside (IPTG; Calbiochem), and the cells were harvested after 4 h. Cells were washed with PBS and resuspended in lysis buffer (300 mM NaCl, 50 mM NaH_2PO_4, 10 mM imidazole, pH 8.0). Lysozyme (Sigma) was added to the suspended cells at a final concentration of 100 ng/ml and incubated on ice for 30 min. The cells were then sonicated (6 × 10 sec) with 10 sec on ice between each cycle. The lysate was clarified by centrifugation (10 000 × *g*, 30 min) at 4°C and analyzed by SDS-PAGE. In IPTG-induced samples, a prominent band with an apparent mobility of ≈25 kDa can be seen that is not present in the uninduced samples (see Supplemental Figure S1A, *left*; all Supplemental Data are available online at www.biolreprod.org). Lysate was incubated with 2 ml of nickel-nitrilotriacetic acid agarose (Qiagen) for 1 h at 4°C. The resin was packed into a column and washed with 16 column volumes of 300 mM NaCl, 50 mM NaH_2PO_4, 20 mM imidazole, pH 8.0. Bound protein was eluted with 300 mM NaCl, 50 mM NaH_2PO_4, 250 mM imidazole, pH 8.0. Protein concentration was determined by bicinchoninic acid (BCA) assay (Pierce), and fractions were analyzed by SDS-PAGE. The prominent band at ≈25 kDa seen in the crude bacterial lysates was highly enriched after affinity purification (see Supplemental Figure S1B). Protein concentrations for mature SPACA7 were calculated from absorbance at 280 nM using an extinction coefficient $E^{1cm}_{1\%}$ of 2.59 (ProtParam [8]). New Zealand White rabbits were immunized with purified SPACA7 to produce polyclonal antiserum (Washington Biotechnology, Inc.).

Affinity Purification of Polyclonal Immunoglobulin. Purified recombinant SPACA7 was coupled to UltraLink Biosupport beads to a density of 3.7 mg/ml resin according to the instruction of the supplier (Thermo Scientific). After coupling, the resin was incubated with 3.0 M ethanolamine, pH 9.0 to quench any unreacted sites. The beads were washed with 0.1 M NaCl, 20 mM 3-(N-Morpholino)propanesulfonic acid (MOPS), pH 7.5 (MBS), and stored at 4°C until use.

The SPACA7-coupled beads were incubated with 100 mM glycine, pH 2.5, and then washed with MBS. Ten milliliters of immune rabbit serum was diluted with 40 ml of MBS, and then 2 ml of SPACA7 beads were added and incubated for 2 h on a rotisserie rotator at 4°C. The mixture was centrifuged (1000 × *g*, 5 min), and the supernatant was removed. The beads were packed into a column and washed with 10 bed volumes (20 ml) of MBS, then 10 bed volumes (20 ml) of 0.5 M NaCl, 20 mM MOPS, pH 7.5. Bound antibody, eluted with 100 mM glycine, pH 2.5, was collected in 2 ml fractions into tubes containing 0.5 ml of 1 M MOPS, pH 7.5, to neutralize the eluate. Fractions were analyzed by SDS-PAGE, and antibody concentrations were calculated from absorbance at 280 nM using an extinction coefficient $E^{1cm}_{1\%}$ of 14.0.

Subcellular Fractionation. Tissues were collected from mice and homogenized in ice-cold MBS supplemented with 10 μg/ml leupeptin, 10 μg/ml antipain, and 1 mM benzamidine using a Dounce homogenizer. The homogenates were centrifuged (800 × *g*, 10 min) to obtain a postnuclear supernatant that was then centrifuged (100 000 × *g*, 1 h, 4°C). The 100 000 × *g* supernatant (soluble fraction) was collected. The 100 000 × *g* pellet was suspended in 100 mM Na_2CO_3, pH 11.5, and incubated on ice for 30 min. The suspension was then centrifuged (100 000 × *g*, 1 h, 4°C). The 100 000 × *g* supernatant (carbonate fraction) was collected. The 100 000 × *g* pellet (membrane fraction) was then extracted into 100 mM NaCl, 20 mM N-Tris (hydroxymethyl)methyl-3-aminopropanesulfonic acid (TAPS), 1% Triton X-100, pH 9.0, on ice for 1 h. The membrane fraction extract was clarified by centrifugation (100 000 × *g*, 1 h, 4°C), and the final pellet was solubilized into NuPAGE LDS sample buffer and heated at 70°C for 10 min. All fractions were stored at −86°C until further analysis.

SDS-PAGE and Western Blotting. Samples were electrophoresed on NuPAGE 4–12% Bis-Tris SDS-polyacrylamide gels with 2-(N-morpholino)ethanesulfonic (MES) SDS running buffer (Invitrogen). GelCode Blue (Pierce) was used for protein staining of gels. Proteins were electroblotted onto Immobilon PVDF membranes (Millipore) using a Transblot SD semidry transfer cell (Bio-Rad). Membranes were blocked with 5% nonfat dry milk powder in Tris-buffered saline (TBS) and then briefly washed with TBS, 0.1% Tween 20 (TBS-T). TBS-T was used for all reagent dilutions and wash steps. SPACA7 antiserum or preimmune serum was used at a 1:30 000 dilution, followed by 25 ng/ml HRP-conjugated goat anti-rabbit IgG. Bound secondary antibodies were detected with SuperSignal West Dura extended duration substrate (Pierce) using a G:BOX Chemi-XR5 gel imaging system (Syngene) equipped with GeneSys v.1.2.5.0 software. To visualize the electroblotted proteins, membranes were stained with 0.1% Coomassie Brilliant Blue R-250 in 50% methanol for 1 min and then destained with 10% acetic acid, 40% methanol, 50% H_2Om for 20 min.

Immunofluorescence Microscopy. Tissues were harvested into ice-cold PBS, fixed with freshly prepared 4% paraformaldehyde in PBS, pH 7.4, for 30 min and then perforated with a 28G½ needle. After overnight fixation, tissues were incubated in PBS for 1 day, 15% sucrose in PBS for 1 day, and then in 30% sucrose in PBS for 1 day. Tissues were then embedded in optimal cutting temperature compound (Sakura Finetek) for 1 day and then frozen in liquid N_2-cooled isopentane. Five-micrometer-thick frozen sections were placed onto slides (Fisherbrand Colorfrost Plus), air-dried, washed with PBS (3 × 5 min), and then permeabilized with PBS, 0.1% Triton X-100, for 1 h. Sections were quenched with 0.1 M glycine, washed with PBS (3 × 5 min), and then blocked with PBS, 10% fetal bovine serum (FBS), for 1 h.

FIG. 1. Amino acid sequence of mouse SPACA7. The 761-bp cDNA predicts a 182-amino-acid polypeptide with a 24-amino-acid signal peptide assuming signal cleavage between Leu^{24} and Gln^{25} (indicated by inverted triangle) (SignalP 4.0; http://www.cbs.dtu.dk/services/SignalP). Asn^{40} fits the consensus sequence for *N*-linked glycosylation (green). The mature polypeptide contains no cysteine or tryptophan residues.

Seminiferous tubule squash preps were prepared as previously described [9]. Briefly, testes were harvested into ice-cold PBS and placed into fixative (1% paraformaldehyde, 0.15% Triton X-100, in PBS, pH 7.4). The tunica albuginea was quickly removed, and seminiferous tubules were separated and cut into ≈3–5-mm-long sections. After 10 min in fixative, several tubule sections were placed onto poly-L-lysine–coated slides (Fisherfinest Superfrost) along with a 30-μl droplet of fixative. The tubules were spaced at least 3–5 mm apart. A coverslip was placed over the tubules and fixative droplet, excess fixative was wiped away, and then a No. 2 pencil eraser was used to press down or ''squash'' the tubules with minimal force. Excess fixative was wiped away, and then the slides were frozen in liquid N_2. Once frozen, the coverslips were removed and then immediately placed into PBS.

Caput epididymal sperm were collected by mincing two caput epididymides into 250 μl of warm HTF, while caudal sperm were collected from the cauda epididymis and vas deferens into 250 μl of warm HTF containing 15 mg/ml of bovine serum albumin (BSA), Cohn fraction V (Equitech-Bio, Inc.). The sperm were incubated at 37°C, 5% CO_2, for 15 min and then washed three times with PBS. Sperm were counted, and 50 000 sperm were placed onto slides, air-dried for 90 min, and then washed once with PBS. Slides were fixed with 4% paraformaldehyde in PBS, pH 7.4, for 10 min; permeabilized with 0.5% Triton X-100 in PBS for 5 min; and then blocked in PBS, 0.5% BSA, overnight.

For staining of tissue sections, the diluent for primary and secondary antibodies and for washing steps was PBS. For staining squash preps, the diluent for primary antibody was PBS, 10% FBS. For secondary antibody and washes, PBS was used. For staining of sperm, the diluent for primary and secondary antibodies and for washing steps was PBS, 0.1% Tween. For tissue sections and sperm, slides were incubated for 1–2 h with SPACA7 antiserum or preimmune serum at a 1:1500 dilution. For squash preps, slides were incubated for 2 h with SPACA7 antiserum or preimmune serum at a 1:1500 dilution and either anti-SYCP3 (1.74 μg/ml) or anti-SYN6 (2.0 μg/ml). After washing, samples were incubated for 1–2 h with secondary antibodies. For SPACA7 staining, FITC-goat anti-rabbit IgG was used at 2.75 μg/ml, while DyLight 594-goat anti-mouse IgG was used at 1.25 μg/ml for SYCP3 and SYN6 staining. Rhodamine-PNA was used at 10 μg/ml to stain the acrosome. Sections were washed and then mounted with Vectashield hard set mounting medium with DAPI. Images were captured using a Nikon E800M microscope equipped with Nikon ACT-1 v.2.62 software. Individual channel images were captured at the same filter and camera settings and later merged in Adobe Photoshop CS5 using the linear dodge blending mode.

Immunoelectron Microscopy. Caudal sperm was collected and capacitated as for immunofluorescence microscopy, washed in ice-cold PBS, and fixed in 4% paraformaldehyde, 1% glutaraldehyde, in PBS, pH 7.2, for 30 min. Sperm were pelleted in 1% low melting point agarose (bioWORLD), and the agarose was allowed to set. Tissues were harvested into ice-cold PBS, fixed in 4% paraformaldehyde, 1% glutaraldehyde, in PBS, pH 7.2, for 30 min, and then perforated with a 28G½ needle. After an additional 1 h of fixation, the tissues were washed with several changes of PBS and then incubated overnight. Tissues or agarose were cut into 1–3-mm pieces and passed through a 70–90% graded ethanol series. Tissues or agarose pieces were incubated in three changes of LR White (Fluka Analytical). A final change of LR White was made before placing tissues into gelatin capsules (Electron Microscopy Services), being careful to exclude air. The capsules were incubated at 50°C for 2 days to polymerize the resin. Tissues or agarose pieces were sectioned at 0.05 μm and dried onto 400-mesh nickel grids. Immunostaining was performed by floating the grids on droplets of staining solutions. The diluent for primary and secondary antibodies and for washing steps was 0.2% BSA, 0.2% normal goat serum, 0.004% fish scale gelatin in PBS, unless otherwise indicated. Grids were quenched on 0.05 M glycine in PBS for 15 min, washed (3 × 5 min), and then incubated on SPACA7 antiserum (1:3000) for 1 h. Grids were washed (3 × 5 min) and incubated for 1 h on goat anti-rabbit IgG 10 nm immunogold conjugate (#EM.GAR10; BBInternational) diluted 1:20. Grids were washed (6 × 5 min), incubated on PBS (2 × 5 min), and postfixed on 2% glutaraldehyde in PBS for 5 min. Finally, grids were cleaned with distilled water (3 × 5 min) and counterstained on Reynold's lead citrate [10] for 5 min. Grids were observed in a Hitachi H7600 transmission electron microscope, and digital images (2000 × 2000 pixels) were captured using an in-line digital camera (Eastman Kodak Co.).

In Vitro Fertilization Assays. Six- to eight-wk-old NSA (CF-1) females were superovulated by intraperitoneal injection of 5 units eCG followed by intraperitoneal injection of 5 units of hCG 48 h later. Both injections were given in the evening prior to the start of the dark cycle. Thirteen hours after hCG injection, egg clutches were collected from the swollen ampullae and then washed and stored in HTF until insemination. For cumulus-free IVF assays, eggs were collected in the same manner but were briefly (≈5 sec) placed into a 200 μl drop of hyaluronidase (75 U/ml) in HTF, 10% FBS, and then immediately washed through six 100-μl drops of HTF. Although cumulus cells remained after the initial exposure to hyaluronidase, the oocytes were cumulus-free after washing through the six wash drops.

Sperm were collected from ICR (CD-1) retired breeders. The cauda epididymides and vas deferens were removed and placed into a 250-μl drop of HTF. The epididymides were gently torn apart, and the contents of the vas deferens were extruded. The sperm were allowed to swim out from the tissue into the HTF for 15 min. Sperm suspension was removed and carefully pipetted below 750 μl of HTF in a 5-ml round-bottom tube. After 45 min, the top 500 μl of HTF containing the highly motile sperm was removed and allowed to capacitate for an additional 30 min, for a total of 90 min. Sperm from this ''swim-up'' fraction were counted, and then 100 μl insemination drops were set up containing 100 000 sperm/mLlin HTF under mineral oil. All incubations were in a 37°C incubator with 5% CO_2.

Affinity-purified anti-SPACA7 IgG and control rabbit IgG (EMD Millipore) were dialyzed against MBS. Antibodies (2–10 μl, 1 mg/ml) were added to the sperm in the insemination drops at a final concentration of 20–100 μg/ml and equilibrated for 30 min. Finally, ≈30 eggs were added to each insemination drop. Four hours after insemination, the oocytes were washed once with HTF, transferred to a 50-μl drop of HTF, and then incubated overnight at 37°C, 5% CO_2. The numbers of two-cell embryos were counted 24 h after insemination.

For real-time visualization after insemination, the drops were viewed under a Zeiss 710 confocal microscope equipped with an incubation chamber set at 37°C and 5% CO_2. Images were acquired every hour for 4 h at 5× magnification while leaving the insemination dishes undisturbed. Another set of IVF experiments were performed under identical conditions, except that after insemination the eggs were transferred with any adherent cumulus cells into 2% glutaraldehyde in 0.1 M sodium cacodylate buffer for 1 h at room temperature. Eggs were washed for 15 min in two changes of 0.1 M sodium cacodylate buffer and postfixed in 1% osmium tetroxide in 0.1 M sodium cacodylate buffer for 1 h at room temperature. Eggs were washed three times for 15 min in distilled water and then dehydrated through a graded ethanol series and then into 100% propylene oxide. The eggs were then transferred into three changes of EMbed-812 resin (Electron Microscopy Sciences) and polymerized for 2 days at 65°C. Polymerized tissues were sectioned at 0.5 μm on a Leica EM UC6 Ultracut Microtome and floated onto drops of 1% toluidine blue in 1% sodium borate at 50°C for 5 min. Stained sections were floated on distilled water, transferred to a glass slide, dried at 50°C, and mounted in VectaMount (Vector Laboratories).

Assessing Acrosome Status of Epididymal Sperm. Caudal epididymal sperm from ICR (CD-1) mice were collected, capacitated, and placed under oil (100 μl, 100 000 sperm/ml) in the identical manner as described for the IVF assays. Samples were taken at various time points before and after addition of anti-SPACA7 IgG (20 μg/ml), control rabbit IgG (20 μg/ml), or vehicle (MBS). Sperm were washed with PBS and then centrifuged onto poly-L-lysine–coated slides using a Cytopro cytocentrifuge. Slides were dried at 37°C, then processed for PNA staining as described above.

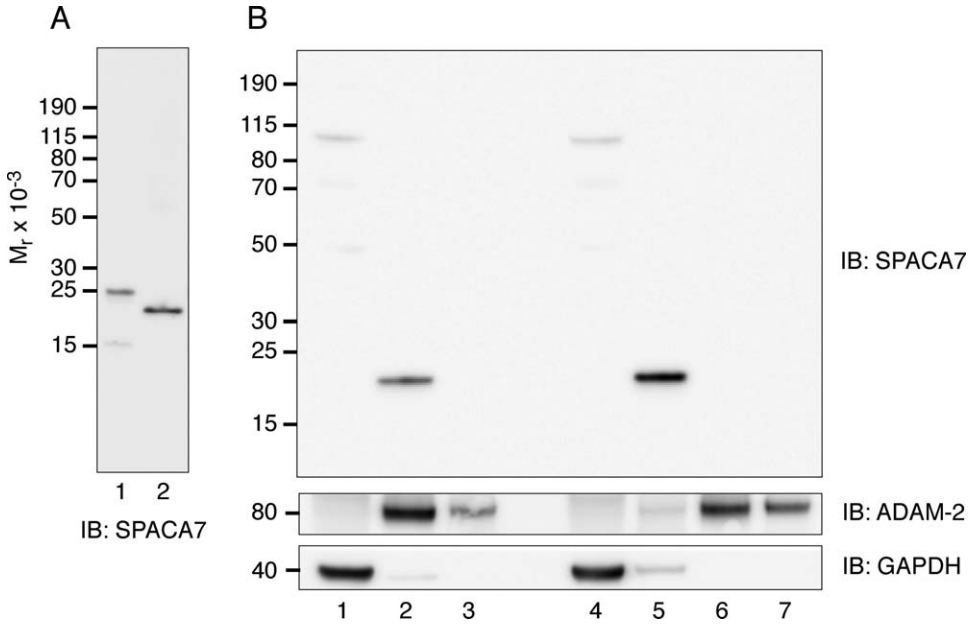

FIG. 2. Characterization of SPACA7 antiserum and subcellular localization of SPACA7. **A**) Recombinant SPACA7 expressed in bacteria (lane 1) and a carbonate fraction of testes (lane 2) were subjected to SDS-PAGE under nonreducing conditions followed by Western blotting with SPACA7 antiserum. **B**) Testes were fractionated into a soluble fraction (lane 1), Triton-soluble membrane fraction (lane 2), and Triton-insoluble membrane fraction (lane 3). Alternately, testes were fractionated into a soluble fraction (lane 4), carbonate fraction (lane 5), Triton-soluble membrane fraction (lane 6), and Triton-insoluble membrane fraction (lane 7) as described in *Methods*. Samples were subjected to SDS-PAGE under nonreducing conditions followed by Western blotting with SPACA7 antiserum. Each lane represents 1.5% of the total fraction. The membranes were stripped and reprobed with anti-ADAM-2, then stripped again and reprobed with anti-GAPDH. A Western blot of an independent subcellular fractionation probed with SPACA7 antiserum or preimmune serum followed by HRP-conjugated goat anti-rabbit IgG is shown in Supplemental Figure S2A.

RESULTS

In Silico Characterization of SPACA7

The gene encoding for mouse SPACA7 resides on chromosome 8 and spans seven exons. The 761-bp cDNA predicts a 182-amino-acid polypeptide with a 24-amino-acid signal peptide assuming signal cleavage between Leu^{24} and Gln^{25} (SignalP 4.0 Server [11]; Fig. 1). Thus, the mature polypeptide has 158 amino acids. It is predicted to have a molecular weight of 17,286.7 Da, a pI of 4.48 (ProtParam [8]), one potential site for N-glycosylation at Asn^{40}, and no cysteine residues. As mentioned above, microarray data reported at BioGPS.org showed that SPACA7 transcripts were detected only in testis. *Spaca7* orthologs are present in other species, including the rat (Gene ID: 689077), cow (Gene ID: 781940), and in various primates, including chimpanzee (Gene ID: 737122) and humans (Gene ID: 122258).

Characterization of Recombinant SPACA7

Recombinant mouse SPACA7 was expressed in bacteria and purified as described in *Methods*. To verify that the purified recombinant protein was SPACA7, samples were resolved by SDS-PAGE, and the gel band was reduced and alkylated before end-stage tryptic digestion. Peptides were extracted from the polyacrylamide and analyzed by LC-MS. The peptide sequences obtained covered the entire construct, including the epitope tag, and showed that the N-terminal methionine was absent. However, the apparent molecular weight based on its mobility in SDS-PAGE is substantially higher than the predicted molecular weight of the recombinant SPACA7, 18 409 Da (after Met removal). To address this discrepancy, the purified SPACA7 was subjected to matrix-assisted laser desorption/ionization time-of-flight mass spectrometry (MALDI-TOF MS; see Supplemental Methods and Supplemental Figure S1C). Major peaks detected at m/z 18 434 and 9219 corresponded to singly and doubly protonated ions derived from the same protein. The slightly greater (26 Da) mass relative to the expected M_r of SPACA7 (18 409 average mass) is likely explained by low-frequency oxidation amino acid side chains. This confirms the expected M_r of expressed SPACA7 and indicates that the slow SDS-PAGE migration of the protein is an intrinsic property of the recombinant polypeptide.

Characterization of SPACA7 Antiserum

New Zealand white rabbits were immunized with purified recombinant SPACA7, and the resulting antiserum was tested by Western blotting of recombinant SPACA7 and testis extracts. As expected, the antiserum also detected recombinant SPACA7 at ≈25 kDa (Fig. 2A, lane 1). In testis extracts, the antiserum detected a single protein species with an apparent molecular weight of ≈17 kDa (Fig. 2A, lane 2). When testis extract were treated with peptide:N-glycosidase, no change in the electrophoretic mobility of SPACA7 was observed (data not shown), indicating that Asn^{40} of SPACA7 is not glycosylated. Therefore, the molecular weight of native SPACA7 estimated from its electrophoretic mobility is consistent with its predicted molecular mass of 17 286.6 Da, assuming that signal peptide cleavage occurs between Leu^{24} and Gln^{25} and that there are no posttranslation modification. The reason that recombinant SPACA7 runs at a higher apparent molecular weight than its molecular mass of 18 434 Da is not certain. One likely possibility is that it is due to the added mass and/or charge conferred by the His_6 tag. Another possibility is that the ≈7–8-kDa difference in the apparent molecular weight

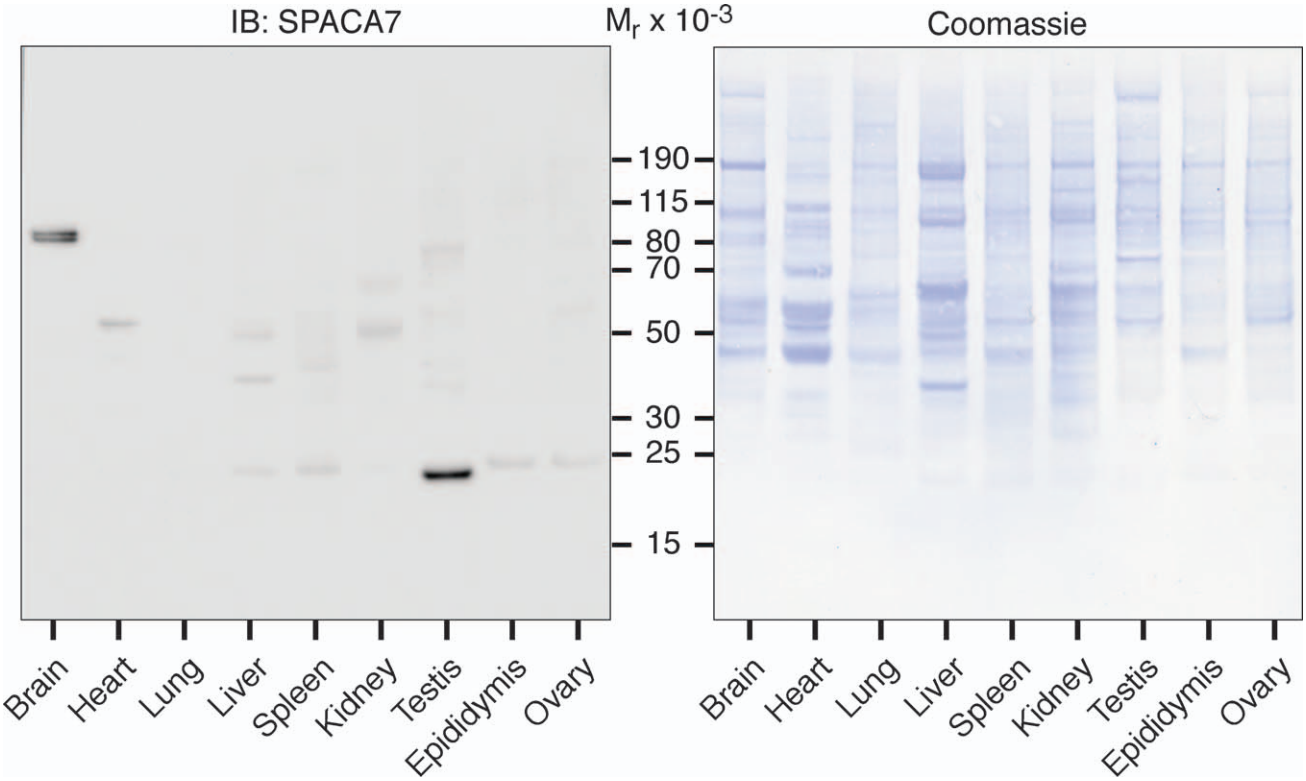

FIG. 3. Expression of SPACA7 in tissues. 100 000 × *g* pellets from tissue homogenates were extracted with 100 mM Na_2CO_3, pH 11.5, and then 10 μg of protein from each tissue were subjected to SDS-PAGE under nonreducing conditions followed by Western blotting with SPACA7 antiserum (left panel). After Western blotting, the membrane was stained with Coomassie Brilliant Blue to show protein content (right panel). A duplicate Western blot probed with preimmune serum followed by HRP-conjugated goat anti-rabbit IgG is shown in Supplemental Figure S2B.

of recombinant and native SPACA7 is due to proteolytic processing of the native SPACA7.

Subcellular Fractionation

Testes were homogenized, subjected to subcellular fractionation, and analyzed by Western blotting with SPACA7 antiserum (Fig. 2B). When testis was processed into a soluble, a Triton-soluble, and a Triton-insoluble membrane fraction, an immunoreactive band at ≈17 kDa was detected only in the Triton soluble membrane fraction (lane 2). However, if the 100 000g pellet from testis was extracted with 100 mM Na_2CO_3, pH 11.5, prior to detergent extraction, SPACA7 was detected only in the carbonate fraction (lane 5) and not in the Triton-soluble membrane fraction (lane 6). SPACA7 was not detected in the soluble fractions (lanes 1 and 4) or the Triton-insoluble material (lanes 3 and 7) from either subcellular fractionation. The minor immunoreactive ≈100-kDa band detected in the soluble fractions (lanes 1 and 4) was also detected when the membrane was probed with preimmune serum (see Supplemental Figure S2A). The nature of this minor species is not known, but it is not a disulfide-linked heterodimer of SPACA7 and another protein because SPACA7 has no cysteine residues.

To validate the fractionation procedures, we probed the membranes for GAPDH and ADAM-2. In both fractionations, GAPDH, a soluble cytosolic protein, was detected mostly in the soluble fraction. Likewise, ADAM-2, a known membrane protein, was detected mostly in the Triton-soluble membrane fractions and not in the carbonate fraction. The extractability of SPACA7 in high-pH sodium carbonate suggests that it may be a peripheral membrane protein or is enclosed within a membrane-bound organelle [12, 13].

Expression of SPACA7 in Tissues

High-throughput gene expression profiling reported at BioGPS.org detected SPACA7 transcripts only in testis. To further support the testis-specific expression of SPACA7, brain, heart, lung, liver, spleen, kidney, testis, epididymis, and ovary were homogenized, and carbonate fractions were prepared and analyzed by Western blotting with SPACA7 antiserum. Out of all of the tissues analyzed, SPACA7 was detected only in testis (Fig. 3). A tightly spaced doublet at ≈80 kDa in brain as well as other weak bands were detected in these blots. However, these were also detected with preimmune serum and are therefore nonspecific (see Supplemental Figure S2B). Similar results were obtained when Triton-soluble membrane fractions were prepared without prior carbonate extraction (data not shown).

Developmental Onset of SPACA7 Expression

To determine at what age SPACA7 expression begins, we analyzed testis extracts from P8, P17, and P21 and in adult mice by Western blotting. We observed that SPACA7 was not detected at P8 and P17 but was detected at P21 and into adulthood (Fig. 4A). The observation that SPACA7 expression begins at P21 is consistent with the first appearance of endogenous *Spaca7* transcripts as reported by Korfanty et al. [5].

To determine which cells in the testes express SPACA7, we next performed immunofluorescence microscopy of testis at these same time points (Fig. 4B). We observed that SPACA7

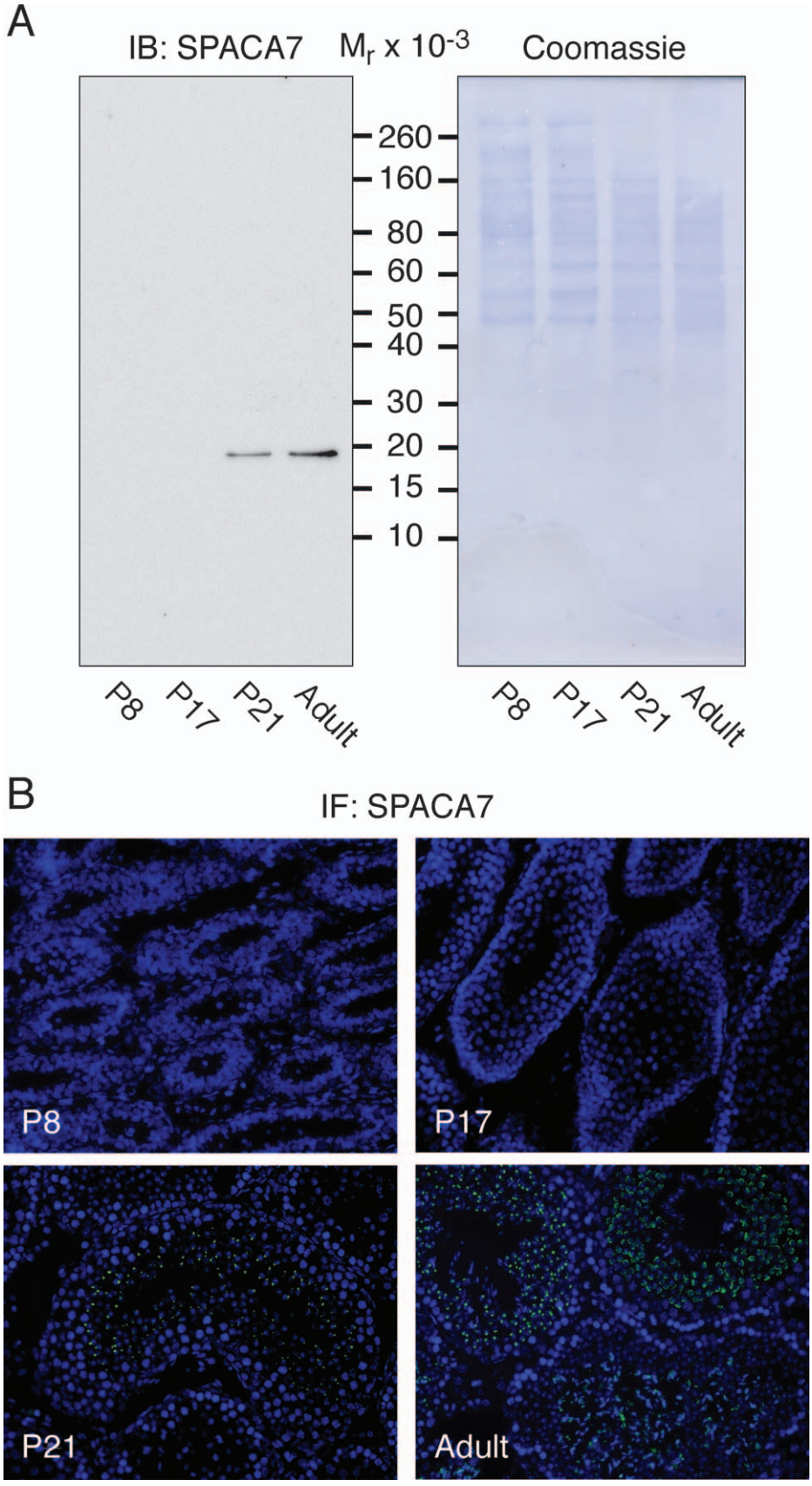

FIG. 4. Developmental onset of SPACA7 expression. **A**) Triton extracts of testes at P8, P17, P21, and adults (10 μg of protein) were subjected to SDS-PAGE under nonreducing conditions followed by Western blotting with SPACA7 antiserum (left panel). After Western blotting, the membrane was stained with Coomassie Brilliant Blue to show protein content (right panel). **B**) Testes sections at the indicated ages were subjected to immunofluorescence microscopy using SPACA7 antiserum (green) and DAPI (blue) as described in *Methods*. Original magnification ×20.

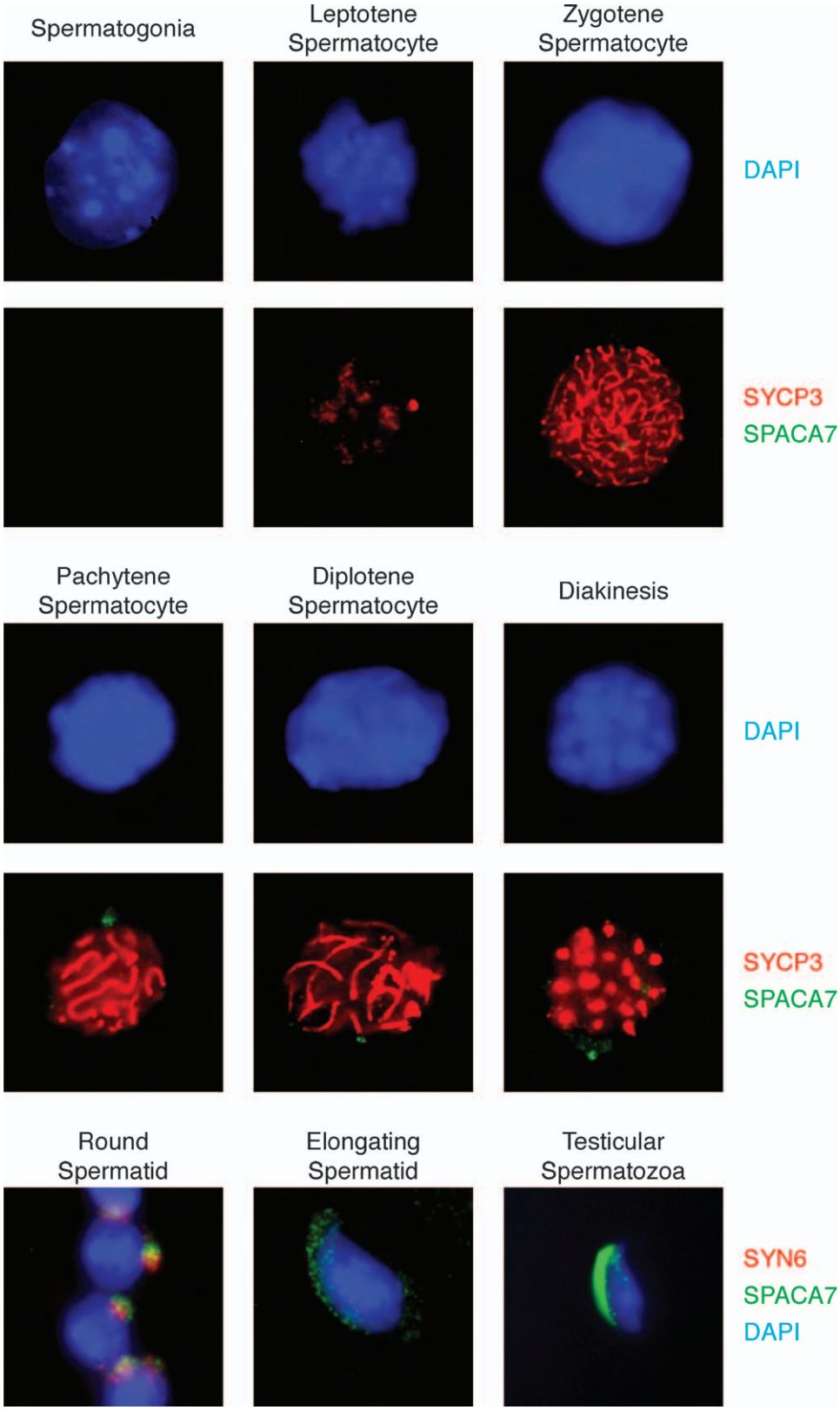

FIG. 5. Developmental onset of SPACA7 expression. Cytologic preps of germ cells from seminiferous tubules were prepared as described in *Methods*. Cells were subjected to immunofluorescence staining for SPACA7 (green), synaptonemal complex protein 3 (SYCP3), or syntaxin 6 (SYN6; red) and DAPI (blue). The number of cells at each period of germ cell development in which SPACA7 was detected as a function of the number of cells examined are as follows: 0 of 38 spermatogonia (0%), 0 of 42 leptotene spermatocytes (0%), 19 of 48 zygotene spermatocytes (40%), 75 of 86 pachytene spermatocytes (87%), 51 of 63 diplotene spermatocytes (81%), and 37 of 44 diakinesis (84%). All round spermatids, elongating spermatids, and testicular spermatozoa examined expressed SPACA7 ($n > 50$). Original magnification ×100.

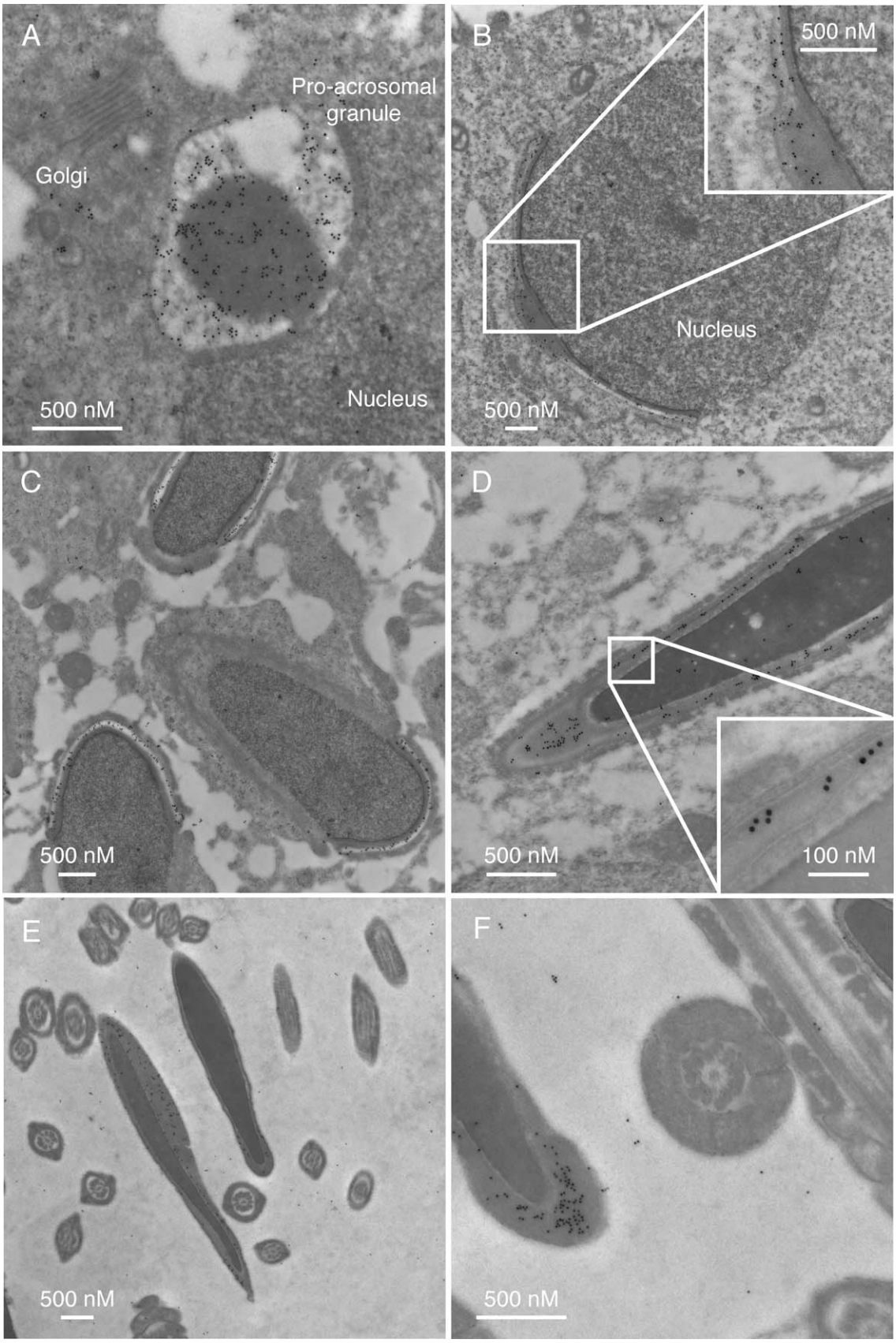

FIG. 6. Immunogold electron microscopy. Immunogold electron microscopy of testes and sperm using SPACA7 antiserum was performed as described in *Methods*. **A**) Round spermatid showing the Golgi stack adjacent to the nascent pro-acrosomal granule and nucleus. **B**) Golgi-phase round spermatid. **C**) Elongating spermatids. **D**) Testicular spermatozoa with gold particles localizing in the acrosomal matrix of the acrosome between the inner and outer acrosomal membrane (inset). **E** and **F**) Caudal epididymal sperm.

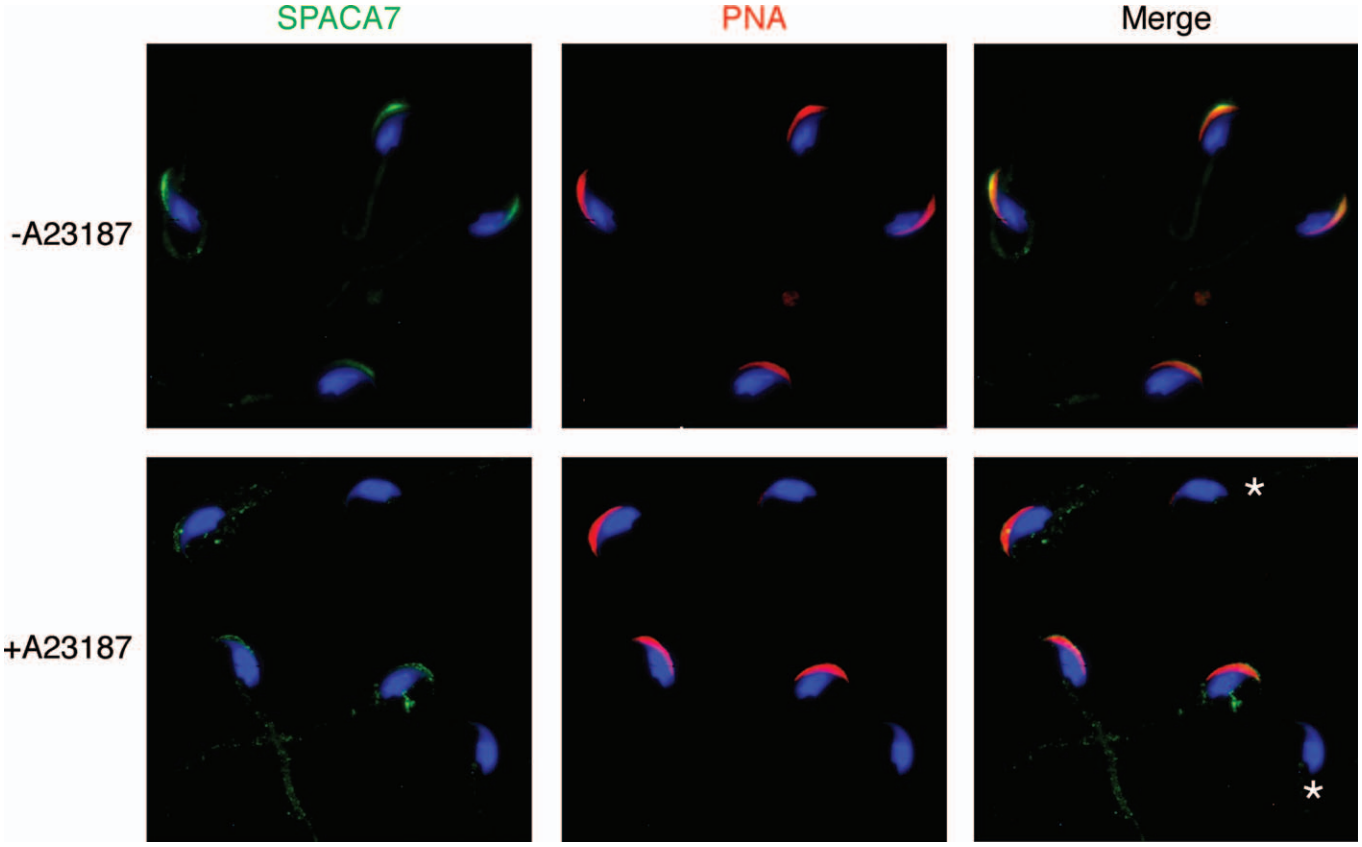

FIG. 7. SPACA7 expression in epididymal sperm. Caudal epididymal sperm were collected as described in *Methods*, then treated with diluent (top panels) or calcium ionophore A23187 (bottom panels). Cells were subjected to immunofluorescence staining for SPACA7 (green), PNA (red), and DAPI (blue). Sperm that have completed acrosome exocytosis as indicated by loss on PNA staining are highlighted by asterisks. Original magnification ×100.

immunostaining was absent at P8 and P17. At P21, immunostaining for SPACA7 was detected in some seminiferous tubules but not others. Staining was seen primarily as a perinuclear spot in developing germ cells located toward the lumen of the tubules. In contrast, in adult testis, SPACA7 is expressed prominently in cells located toward the lumen of all tubules. However, the staining pattern varies from one tubule to the next. One pattern is that of the perinuclear spot, such as that observed at P21. Another looks like the developing germ cells have a cap of SPACA7 immunoreactivity, while in yet a third pattern, the lumenally oriented germ cells have a crescent pattern suggestive of acrosomal staining of elongating spermatids and/or spermatozoa.

To determine more precisely when SPACA7 expression begins, germ cells from seminiferous tubule squash preps were stained with SPACA7 antiserum (Fig. 5). We observed that spermatogonia did not express SPACA7. However, as germ cells progress through meiosis I, as indicated by the staining patterns of synaptonemal complex protein 3 (SYCP3), SPACA7 is weakly detected in a perinuclear location in zygotene and pachytene spermatocytes. As the germ cells complete meiosis and become haploid round spermatids, the expression of SPACA7 increases substantially and persists. At the Golgi phase of spermiogenesis, SPACA7 staining appears as a round perinuclear spot adjacent to the Golgi apparatus, marked by syntaxin 6 (SYN6). As spermatids elongate and become spermatozoa, the expression pattern of SPACA7 appears to be associated with the acrosome, and the SYN6 Golgi marker disappears.

Immunoelectron Microscopy

The acrosome is comprised of an outer acrosomal membrane, matrix, and inner acrosomal membrane. In order to determine precisely where SPACA7 localized, we performed immunogold electron microscopy. In round spermatids, we observe abundant gold particles localized to the perinuclear proacrosomal granule but not to the adjacent Golgi stack (Fig. 6A). As round spermatid mature into elongated spermatids and spermatozoa, abundant gold particles are seen within the developing acrosome (Fig. 6, B and C). High-magnification images of the head of testicular spermatozoa clearly show that abundant gold particles are localized between the inner and outer acrosomal membranes and not on the exterior surface of the sperm (Fig. 6D, inset).

SPACA7 Expression in Epididymal Sperm

We next examined expression of SPACA7 in epididymal sperm. In sperm from the caput, we observed SPACA7 staining that colocalizes with PNA staining overlying the sperm head (data not shown). This acrosome-like staining pattern remains as the spermatozoon matures and transits to the cauda epididymis (Fig. 7, top panels). In addition, immunogold electron microscopy showed that SPACA7 is localized only to the acrosome and not to other regions of caudal sperm (Fig. 6, E and F). Finally, when caudal sperm are stimulated with calcium ionophore A23187 (5 μM, 30 min, 37°C) to trigger acrosome exocytosis, SPACA7 staining is lost on sperm that have completed acrosome exocytosis, as indicated by loss on PNA staining (asterisks, Fig. 7, bottom right panel).

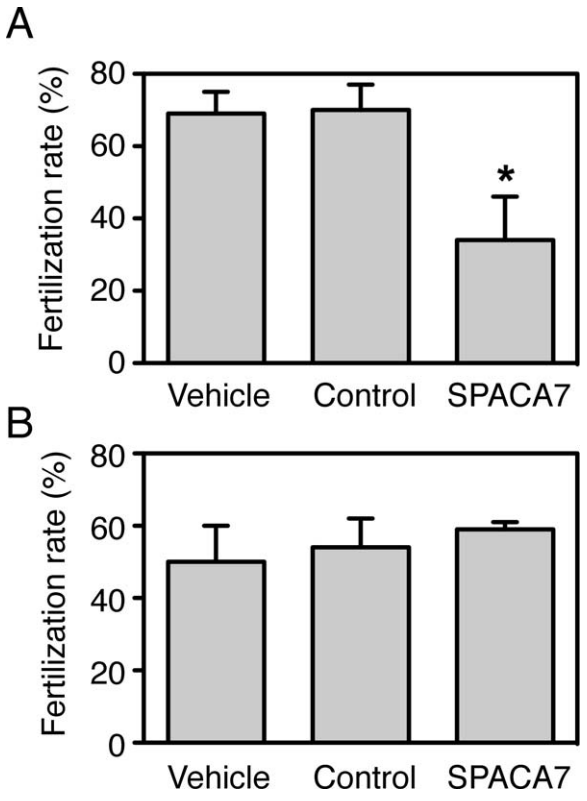

FIG. 8. IVF assays. **A**) Caudal sperm were capacitated for 90 min, then incubated with vehicle, control rabbit IgG, or anti-SPACA7 IgG. After 30 min, clutches of cumulus-intact metaphase II eggs were added to the drops, and the percentage of two-cell embryos was scored 24 h after insemination. The number of eggs scored in each experimental group were vehicle (25 ± 7), control IgG (23 ± 4), SPACA7 IgG (30 ± 7; mean ± SEM, n = 4). **B**) IVF assays were performed as in **A**, except that the cumulus was removed by brief exposure to hyaluronidase prior to insemination (n = 3). The number of eggs scored 24 h after insemination in each experimental group were vehicle (22 ± 5), control IgG (19 ± 3), and SPACA7 IgG (20 ± 1). Results are expressed as mean ± SEM. Statistical differences between groups were tested using unpaired, two-tailed *t*-tests with equal sample variance and an $\alpha \leq 0.05$. An asterisk indicates $P < 0.05$ compared to control IgG and vehicle.

In Vitro Fertilization Assays

Localization of SPACA7 within the acrosome suggests that it may play a role in fertilization. To address this possibility, a series of IVF assays were performed. Caudal sperm were capacitated for 90 min and then incubated with affinity-purified anti-SPACA7 IgG, an equivalent amount of control rabbit IgG, or vehicle. After 30 min, clutches of ≈25 cumulus-intact eggs were added to the drops, and the percentage of two-cell embryos was scored 24 h after insemination. We observed that 20 μg/ml of anti-SPACA7 IgG decreased the fertilization rate by ≈51% compared to control IgG (n = 4, $P < 0.05$; Fig. 8A). However, a higher concentration of anti-SPACA7 IgG did not further decrease fertilization rates. At 100 μg/ml, anti-SPACA7 IgG decreased the fertilization rate by ≈48% compared to control IgG ($P < 0.001$). Under the later conditions, the fertilization rate was 82 ± 6% with vehicle, 87 ± 4% with control IgG, and 45 ± 4% with anti-SPACA7 IgG (mean ± SEM, n = 5). When sperm were incubated with anti-SPACA7 IgG under the same condition as in IVF assays but in the absence of eggs, we observed no differences in the percentage of acrosome-intact (PNA positive) sperm as a function of time compared to control IgG or vehicle alone (see Supplemental Figure S3).

During these IVF experiments, it was noted that the cumulus mass surrounding eggs that were inseminated in the presence of anti-SPACA7 IgG appeared relatively intact compared to controls 4 h after insemination. To document this more carefully, a second set of IVF experiments were performed under identical conditions, except that the egg clutches were photographed before and after insemination. We observed that the cumulus appeared intact when eggs were inseminated in the presence of anti-SPACA7 IgG compared to controls at 4 h after insemination (Fig. 9A). This observation was confirmed when examined at higher resolution in toluidine blue-stained resin sections (Fig. 9B).

We next examined if the anti-SPACA7 IgG could inhibit fertilization of cumulus-free eggs. Therefore, a third set of IVF experiments was performed in which the cumulus was removed by brief exposure to hyaluronidase prior to insemination. No difference in fertilization rates was observed in the presence of anti-SPACA7 IgG, control IgG, or vehicle alone (Fig. 8B).

Finally, we examined if anti-SPACA7 IgG affected the ability of sperm to penetrate the cumulus oophorus. In these experiments, cumulus-oocyte complexes were inseminated exactly as in the cumulus-intact IVF assays described above but were transferred into 2% glutaraldehyde fixative at various times after insemination. The number of sperm heads within 20 μm of the egg were then counted manually in sections in which the eggs were sectioned through the equator as indicated by a thin, sharply defined zona pellucida, as illustrated in Fig. 9B and Supplemental Figure S4. We observed no difference in sperm penetration in the presence of anti-SPACA7 IgG and control IgG at 5–20 min after insemination (two-way analysis of variance, $P = 0.331$; Fig. 10).

DISCUSSION

We developed a polyclonal antibody to study the expression and function of mouse SPACA7. Western blotting of extracts from various tissues detected SPACA7 protein expression only in the testis, and SPACA7 was detected in testis beginning at P21 and into adulthood. This temporal expression pattern was also observed using immunofluorescence staining of testis. At first, this suggested to us that SPACA7 expression may be restricted to postmeiotic germ cells because P21 coincides with the first appearance of round spermatids during the first wave of spermatogenesis [14]. However, immunofluorescence staining of germ cells from seminiferous tubule squash preps showed that SPACA7 was weakly detected somewhat earlier in zygotene and pachytene spermatocytes. This onset of expression coincides with the start of acrosomal biogenesis as well as the onset of expression of acrosomal proteins [15–19].

In adult mice, immunofluorescence staining of testis section showed that SPACA7 was detected on lumenally oriented germ cells in a crescent-like pattern suggestive of acrosomal staining. Immunofluorescence staining of round spermatids from squash preps clearly showed that SPACA7 was localized to a perinuclear spot adjacent to the Golgi and to the acrosome in elongating spermatids and spermatozoa. These findings were further extended using immunogold electron microscopy that demonstrated conclusively that SPACA7 expression was restricted to the proacrosomal granule of round spermatids and the acrosome of testicular spermatozoa. In addition, high-resolution immunogold images clearly show that SPACA7 resides within the acrosome and is not expressed on the plasma membrane overlying the acrosome. These finding are entirely consistent with our subcellular fractionation studies showing

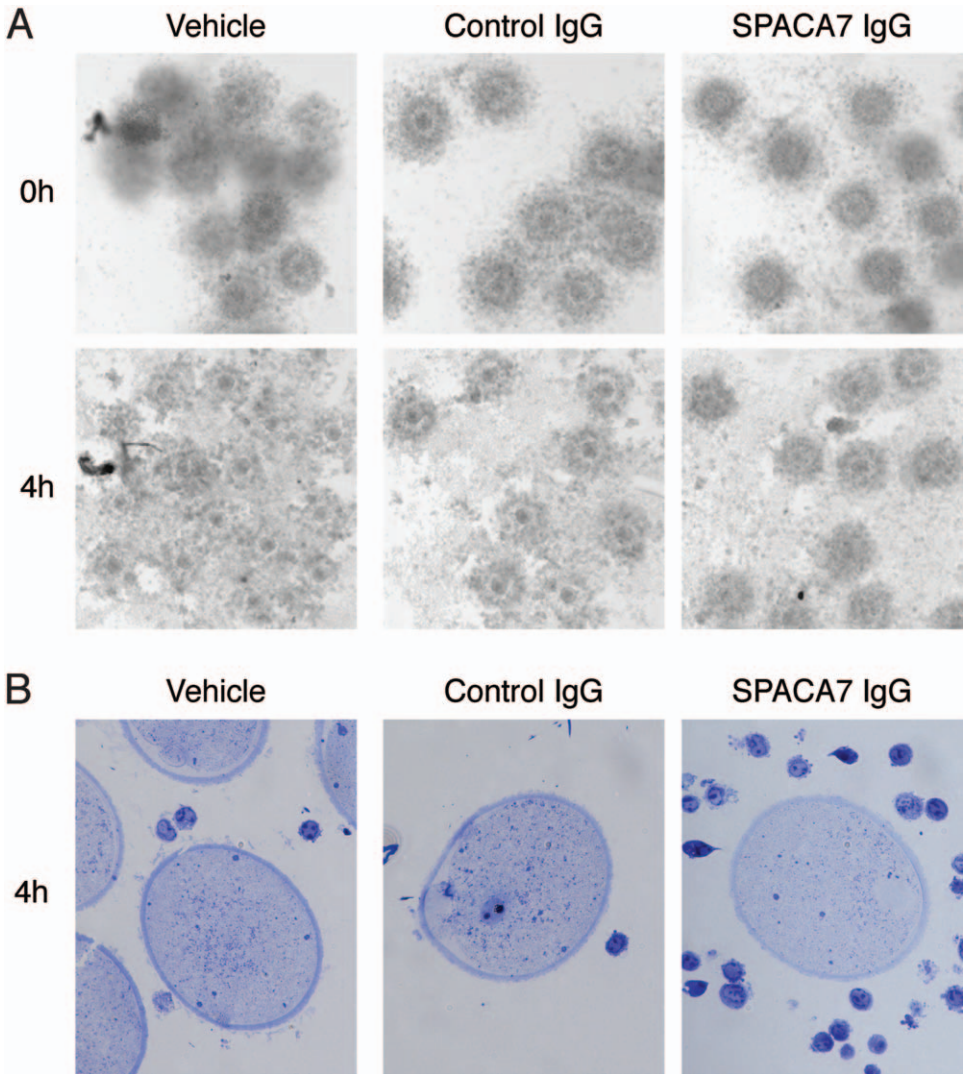

FIG. 9. Cumulus dispersal during IVF assays. IVF assays were performed in the presence of vehicle (left panels), control rabbit IgG (middle panels), or anti-SPACA7 IgG (right panels) as described in Figure 8A. **A**) Cumulus-intact eggs were left undisturbed for 4 h after insemination and then photographed. Original magnification ×20. **B**) Cumulus-intact eggs were left undisturbed for 4 h after insemination and then transferred with any adherent cumulus cells into glutaraldehyde fixative and toluidine blue-stained resin section prepared. The data shown are representative of three independent experiments. Original magnification ×100.

that SPACA7 was sedimented at 100 000 × *g* but could be extracted from the 100 000 × *g* pellet with high-pH sodium carbonate [12, 13]. Finally, immunofluorescence and immunogold electron microscopy show that SPACA7 is retained within the acrosome of caudal sperm and is released upon the acrosome reaction.

To assess the potential role of SPACA7 in fertilization, a series of IVF experiments were performed in the presence of anti-SPACA7 IgG. We observed that 20 μg/ml of anti-SPACA7 IgG significantly inhibited fertilization of cumulus-intact eggs by ≈50%. Inhibition of fertilization was not enhanced at 100 μg/ml of anti-SPACA7 IgG. This could be due to two non-mutually exclusive possibilities. One possibility is that the inhibitory action of the SPACA7 antibody is diffusion limited. At insemination the antibody is present, but the antigen is not accessible until after individual sperm undergo acrosome exocytosis. This would allow time for the SPACA7 release to have its biological effect(s) before it can be inhibited by antibody. Alternately, it could be that the SPACA7 antibody is only partially inhibitory of SPACA7 function.

Interestingly, inhibition of fertilization by SPACA7 antibody coincided with a dramatic inhibition of cumulus dispersal. At the same time, SPACA7 antibody treatment did not result in a significant inhibition or delay of sperm penetration of the cumulus oophorus that we could detect. However, it is possible that our methodology lacked sufficient temporal and spatial resolution to detect a small but biologically relevant inhibition of sperm penetration. Anti-SPACA7 IgG did not affect the rate of spontaneous acrosome reaction, nor did it have any impact of the fertilization of cumulus-free oocytes. These later observations strongly support the conclusion that inhibition of fertilization by anti-SPACA7 IgG was not due to a direct deleterious effect of anti-SPACA7 IgG on the sperm or the egg. Furthermore, these data argue that SPACA7 does not play a direct role in sperm-egg binding or gamete fusion. The finding that anti-SPACA7 IgG inhibits neither sperm penetration nor fertilization in the absence of the cumulus suggests that SPACA7 may facilitate fertilization by triggering elaboration of a factor(s) from cumulus cells that enhances the fertilization competence of sperm. Additional studies will be needed to explore this

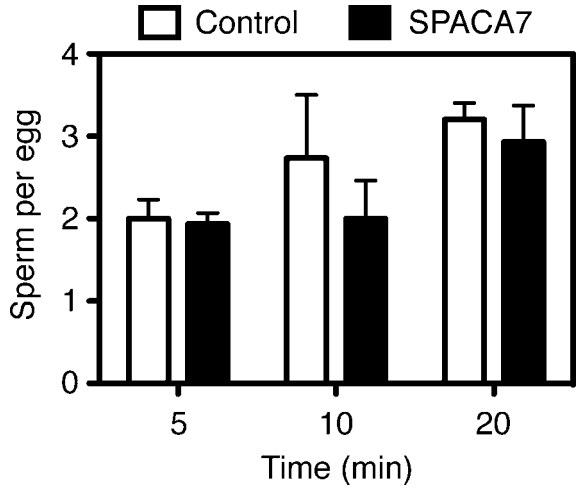

FIG. 10. Sperm penetration of the cumulus oophorus. Cumulus-oocyte complexes were inseminated as described in Figure 8A but were fixed at various times after insemination and toluidine blue-stained resin sections prepared. The number of sperm heads within 20 μm of the egg were counted in which the egg were sectioned through the equator for five eggs from each of three independent inseminations. Results are expressed as the mean ± SEM. Statistical differences between the treatment groups were tested by two-way analysis of variance. There was no statistical difference in between the two treatment groups ($P = 0.331$).

possibility. This study is the first to document the developmental expression and subcellular localization of endogenous SPACA7 and its role in mammalian fertilization.

The importance of the cumulus in fertilization is well documented. Not only are in vitro fertilization rates reduced by cumulus removal, but the cumulus also participates in stimulating sperm motility and/or in promoting the acrosome reaction [20–22]. Hyaluronidases have long been thought to be important for the ability of sperm to efficiently penetrate the hyaluronan-rich cumulus matrix. To date, only two catalytically active sperm hyaluronidases have been convincingly demonstrated in the mouse, SPAM1 (i.e., PH-20) and HYAL5 [23–26]. Both are expressed as glycosylphosphatidylinositol-anchored proteins. SPAM1 is localized on the sperm plasma membrane and is partially retained on acrosome-reacted sperm [24]. HYAL5 is thought to reside on both the plasma membrane and the acrosomal membrane and is released upon the acrosome reaction [23]. Although *Spam1*$^{-/-}$ and *Hyal5*$^{-/-}$ males are fully fertile, recent studies revealed that *Spam1*-null sperm are defective in their ability to enter and penetrate the cumulus mass in vitro, whereas *Hyal5*-null sperm are indistinguishable from wild-type sperm in this regard [27].

The mechanism by which SPACA7 accelerates cumulus dispersal is uncertain. It is unlikely that SPACA7 has hyaluronidase activity because it has no sequence similarity to known hyaluronidases and the predicted size of the mature 158-residue SPACA7 protein is considerably smaller than the catalytic domains of mammalian hyaluronidases, such as SPAM1 and HYAL5. Nevertheless, we incubated cumulus oocyte complexes for 4 h with up to 0.4 mg/ml of purified recombinant mouse SPACA7 expressed in *E. coli* and observed no impact on cumulus dispersal compared to the same concentration of ovalbumin or vehicle alone (Edward Nguyen; unpublished observation). This observation suggests that SPACA7 does not have hyaluronidase activity and that it does not otherwise directly affect cumulus dispersal. However, this conclusion should be considered tentative because even though SPACA7 lacks cysteine residues, we cannot be certain that the recombinant protein is processed and folded in a native conformation. Therefore, it remains possible that native SPACA7 has hyaluronidase-like activity or that it may indirectly augment the activity of SPAM1 and/or HYAL5. These possibilities require further study.

Our understanding of spermatogenesis, sperm maturation and capacitation, and fertilization has expanded greatly in recent years. However, continued progress in understanding the complex biochemical events surrounding these processes will require studies on the many proteins whose function remains unknown and/or poorly characterized, like the studies we report here.

ACKNOWLEDGMENT

We gratefully acknowledge Dr. Roberto Pezza (Oklahoma Medical Research Foundation) for helpful technical advice on performing seminiferous tubule squash preps, Dr. Mike Kinter (Oklahoma Medical Research Foundation) for technical assistance with LC/MS, and Drs. Chris West and Christa Feasley (University of Oklahoma Health Sciences Center) for assistance with MALDI-TOF MS.

REFERENCES

1. Neill JD (ed.). Knobil and Neill's Physiology of Reproduction. St. Louis, MO: Academic Press; 2006.
2. Schultz N, Hamra FK, Garbers DL. A multitude of genes expressed solely in meiotic or postmeiotic spermatogenic cells offers a myriad of contraceptive targets. Proc Natl Acad Sci U S A 2003; 100:12201–12206.
3. Wu C, Orozco C, Boyer J, Leglise M, Goodale J, Batalov S, Hodge CL, Haase J, Janes J, Huss JW III, Su AI. BioGPS: an extensible and customizable portal for querying and organizing gene annotation resources. Genome Biol 2009; 10:R130.
4. BioGPS.org. http://biogps.org/gene/78634. Accessed 3 December 2013,
5. Korfanty J, Toma A, Wojtas A, Rusin A, Vydra N, Widlak W. Identification of a new mouse sperm acrosome-associated protein. Reproduction 2012; 143:749–757.
6. Vydra N, Winiarski B, Rak-Raszewska A, Piglowski W, Mazurek A, Scieglinska D, Widlak W. The expression pattern of the 70-kDa heat shock protein Hspa2 in mouse tissues. Histochem Cell Biol 2009; 132: 319–330.
7. Ouyang YB, Crawley JTB, Aston CE, Moore KL. Reduced body weight and increased postimplantation fetal death in tyrosylprotein sulfotransferase-1-deficient mice. J Biol Chem 2002; 277:23781–23787.
8. Gasteiger E, Hoogland C, Gattiker A, Duvaud S, Wilkins MR, Appel RD, Bairoch A. Protein identification and analysis tools on the ExPASy Server. In: Walker JM (ed.), The Proteomics Protocols Handbook. Totowa, NJ: Humana Press; 2005:571–607.
9. Bisig CG, Guiraldelli MF, Kouznetsova A, Scherthan H, Hoog C, Dawson DS, Pezza RJ. Synaptonemal complex components persist at centromeres and are required for homologous centromere pairing in mouse spermatocytes. PLoS Genet 2012; 8:e1002701.
10. Reynolds ES. The use of lead citrate at high pH as an electron-opaque stain in electron microscopy. J Cell Biol 1963; 17:208–212.
11. Petersen TN, Brunak S, von Heijne G, Nielsen H. SignalP 4.0: discriminating signal peptides from transmembrane regions. Nat Methods 2011; 8:785–786.
12. Howell KE, Palade GE. Hepatic Golgi fractions resolved into membrane and content subfractions. J Cell Biol 1982; 92:822–832.
13. Fujiki Y, Hubbard AL, Fowler S, Lazarow PB. Isolation of intracellular membranes by means of sodium carbonate treatment: application to endoplasmic reticulum. J Cell Biol 1982; 93:97–102.
14. Bellvé AR, Cavicchia JC, Millette CF, O'Brien DA, Bhatnagar YM, Dym M. Spermatogenic cells of the prepuberal mouse: isolation and morphological characterization. J Cell Biol 1977; 74:68–85.
15. Anakwe OO, Gerton GL. Acrosome biogenesis begins during meiosis: evidence from the synthesis and distribution of an acrosomal glycoprotein, acrogranin, during guinea pig spermatogenesis. Biol Reprod 1990; 42: 317–328.
16. Abou-Haila A, Tulsiani DR. Mammalian sperm acrosome: formation, contents, and function. Arch Biochem Biophys 2000; 379:173–182.
17. Hao Z, Wolkowicz MJ, Shetty J, Klotz K, Bolling L, Sen B, Westbrook VA, Coonrod S, Flickinger CJ, Herr JC. SAMP32, a testis-specific, isoantigenic sperm acrosomal membrane-associated protein. Biol Reprod 2002; 66:735–744.

18. Moreno RD, Alvarado CP. The mammalian acrosome as a secretory lysosome: new and old evidence. Mol Reprod Dev 2006; 73:1430–1434.
19. Buffone MG, Foster JA, Gerton GL. The role of the acrosomal matrix in fertilization. Int J Dev Biol 2008; 52:511–522.
20. Yanagimachi R. Mammalian fertilization, In: Knobil E, Neill JD (eds.), The Physiology of Reproduction, vol. 1, 2nd ed. New York: Raven Press; 1994:189–317.
21. Florman HM, Ducibella T. Fertilization in mammals. In: Neill JD (ed.), The Physiology of Reproduction, vol. 1, 3rd ed. San Diego, CA: Elsevier; 2006:55–112.
22. Jin M, Fujiwara E, Kakiuchi Y, Okabe M, Satouh Y, Baba SA, Chiba K, Hirohashi N. Most fertilizing mouse spermatozoa begin their acrosome reaction before contact with the zona pellucida during in vitro fertilization. Proc Natl Acad Sci U S A 2011; 108:4892–4896.
23. Kim E, Baba D, Kimura M, Yamashita M, Kashiwabara S, Baba T. Identification of a hyaluronidase, Hyal5, involved in penetration of mouse sperm through cumulus mass. Proc Natl Acad Sci U S A 2005; 102: 18028–18033.
24. Baba D, Kashiwabara S, Honda A, Yamagata K, Wu Q, Ikawa M, Okabe M, Baba T. Mouse sperm lacking cell surface hyaluronidase PH-20 can pass through the layer of cumulus cells and fertilize the egg. J Biol Chem 2002; 277:30310–30314.
25. Myles DG, Primakoff P. Why did the sperm cross the cumulus? To get to the oocyte: functions of the sperm surface proteins PH-20 and fertilin in arriving at, and fusing with, the egg. Biol Reprod 1997; 56:320–327.
26. Lin Y, Mahan K, Lathrop WF, Myles DG, Primakoff P. A hyaluronidase activity of the sperm plasma membrane protein PH-20 enable sperm to penetrate the cumulus cell layer surrounding the egg. J Cell Biol 1994; 125:1157–1163.
27. Kimura M, Kim E, Kang W, Yamashita M, Saigo M, Yamazaki T, Nakanishi T, Kashiwabara S, Baba T. Functional roles of mouse sperm hyaluronidases, HYAL5 and SPAM1, in fertilization. Biol Reprod 2009; 81:939–947.